11ᵗʰ International Congress on Metallurgy & Materials SAM/CONAMET 2011.

Effect of temperature on the crevice corrosion resistance of Ni-Cr-Mo alloys as engineered barriers of nuclear repositories

E. C. Hornus[a], M. A. Rodríguez[a,b,c] *

[a]Instituto Sabato, UNSAM / CNEA.
[b]Gerencia Materiales, Centro Atómico Constituyentes, CNEA.
[c]CONICET

Abstract

Deep geological disposal is the strongest alternative to the disposal of high level nuclear waste. Alloys 625, C-22, C-22HS and HYBRID-BC1 are considered among candidates as engineered barriers of nuclear repositories. Localized corrosion, like crevice or pitting corrosion, is one of the most important degradation processes that will limit the lifetime of containers. The susceptibility to crevice corrosion is measured by the value of the repassivation potential (E_{CO}). The objective of the present work is to assess the effect of temperature on the crevice corrosion resistance of these alloys.
Alloy HYBRID-BC1 was the most resistant to chloride-induced crevice corrosion, followed by alloys C-22HS, C-22 and 625. E_{CO} showed a linear decrease with temperature. There is a temperature above which E_{CO} does not decrease anymore, reaching a minimum value. This E_{CO} value is a strong parameter for assessing the localized corrosion susceptibility of a material in a long term timescale, since it is independent of temperature, chloride concentration, crevice mechanism, crevice gap and type of crevice formers.

Key words: crevice corrosion, repassivation potential, temperature, nickel-based alloys

* Martín A. Rodríguez. Tel.: +54-116-772-7353; fax: +54-116-772-7362.
E-mail address: maalrodr@cnea.gov.ar.
* Edgar C. Hornus. Tel.: +54-116-772-7353; fax: +54-116-772-7362.
E-mail address: hornus@cnea.gov.ar.

1. Introduction

Deep geological disposal is the strongest alternative to the disposal of high level nuclear waste (Whiterspoon and Bodvarsson, 2001). Geological repositories are based on the multi-barrier principle, which involves a series of engineered and natural barriers to isolate the waste from the biosphere. The waste containers are the main engineered barrier. Due to its excellent resistance to general and localized corrosion, nickel-based alloys are considered for the fabrication of the outer shell of the high level nuclear waste containers (Gras, 2002). The study of the effect of temperature on the corrosion properties of the alloy is important since during the projected 10.000-year service life, the containers will pass through a temperature gradient caused by the heat generated from radioactive decay. For the construction of the containers the selected materials should meet the requirements of corrosion resistance, mechanical strength, good heat dissipation and stability against heat and radiation. Localized corrosion, like crevice or pitting corrosion, is one of the most important degradation processes that will limit the lifetime of containers. The growth of a pit generates a morphology that is essentially a crevice, so active pits and crevices are basically identical. As mentioned above, the phenomenological aspects of pitting apply equally to crevice corrosion. However, crevice corrosion is more likely since it is stabilized in occluded regions at lower potentials than pitting corrosion (Szklarska-Smialowska, 2005; Combrade, 2000; Galvele and Duffó, 2006; Fontana, 1986). The crevices may occur due to the presence of deposits, corrosion products, etc (Fontana, 1986). The crevice corrosion susceptibility of an alloy in a given environment is measured by the value of the repassivation potential (Rebak, 2000). The lower is E_{CO}, the more aggressive is the environment (Szklarska-Smialowska, 2005).

The temperature of the containers will increase reaching a peak due to the heat dissipation from the waste (Whiterspoon and Bodvarsson, 2001). It is shown in the literature that temperature has a strong effect on crevice corrosion properties of nickel-based alloys and stainless steels. It has been reported that there is approximately a linear relationship between the repassivation potential and the temperature. The repassivation potential decreases as the temperature increases (Evans et al., 2005). The critical temperature above which localized corrosion may occur varies between 30 °C and 60 °C for Ni-Cr-Mo alloys. This parameter may differ substantially depending on the experimental method employed (Evans et al., 2005). A few works on the influence of temperature in crevice corrosion are reported. Some authors argue that once the crevice corrosion initiates at a given temperature, it may propagate at lower temperatures. It is indicated that temperature has a similar effect to potential on the crevice corrosion susceptibility (Valen et al., 1995).

The objective of this work was to assess the effect of temperature on the crevice corrosion resistance of selected Ni-Cr-Mo alloys.

2. Experiment

The chemical composition of the alloys in weight percent are listed in Table 1.
The crevice corrosion repassivation potential was determined by the Potentiodynamic-Galvanostatic-Potentiodynamic (PD-GS-PD) method. This is a modification of the Tsujikawa-Hisamatsu Electrochemical (THE) method (ASTM G 192) (Evans et al., 2005; Mishra and Frankel, 2008; Rincón Ortíz et al., 2010). It consists of three stages:

1)   A potentiodynamic polarization in the anodic direction until reaching an anodic current of 30-300 μA (scan rate 0.167 mV/s).

2)   Application of a constant anodic current of 30-300 μA for 2 hours.

3)   Potentiodynamic polarization in the cathodic direction, from the previous potential until alloy repassivation has been reached (scan rate 0.167 mV/s).

The corrosion potential was measured for 15 minutes and a cathodic pretreatment of 5 min at 50 μA was performed before each test.

Table 1. Chemical composition of the tested alloys in weight percent

Alloy	Ni	Cr	Mo	W	Fe	Co	Si	Mn	C	V	Al	B	Cb+Ta
625	62	21	9	0	5	1	0.5	0.5	0.1	0	0.4	0	3.7
C-22	56	22	13	3	3	2.5	0.08	0.5	0.01	0.35	0	0	0
C-22HS	61	21	17	1	2	1	0.08	0.8	0.01	0	0.5	0.006	0
HYBRID-BC1	62	15	22	0	2	0	0.08	0.25	0.01	0	0.5	0	0

Prism crevice assemblies (PCA) specimens were used in the crevice corrosion tests. They were fabricated based on ASTM G 48, 2003 and contained 24 artificially creviced spots formed by a ceramic washer (crevice former) wrapped with a PTFE tape (ASTM G192-08, 2008). The total surface area of the PCA specimen immersed in the electrolyte was 14 cm^2. The applied torque was 5 N-m. The specimens had a finished grinding of SiC abrasive paper number 600 and they were degreased in acetone and washed in distilled water. Tests were performed in duplicate or triplicate. Experiments were conducted at temperatures ranging from 20 °C to 100 °C in 5 mol/L Calcium Chloride ($CaCl_2$) electrolytes. Tests were performed at air pressure.

The general corrosion of the tested alloys was studied in hydrochloric acid (HCl) solutions simulating the conditions within an active crevice. Prismatic specimens were used. The total surface area of the prismatic specimen immersed in the electrolyte was 10 cm^2. All the specimens had a finished grinding of SiC abrasive paper number 600 and they were degreased in acetone and washed in distilled water. Polishing was performed 1 hour prior to testing. The corrosion potential (E_{CORR}) was monitored for 2 hours of each alloy in 1 and 3 mol/L HCl for eight different temperatures (30 °C-100 °C).

Electrochemical tests were conducted in a one-liter, three-electrode vessel. The temperature of the solution was controlled by immersing the cell in a water bath, which was kept at a constant temperature. Nitrogen was purged through the solution 1 hour prior to testing and it was continued throughout the entire test. The reference electrode was a saturated calomel electrode (SCE), which has a potential of 0,242 V more positive than the Standard Hydrogen Electrode (SHE) at room temperature. The counter electrode consisted of a platinum foil spot-welded to a platinum wire (with a total area of 50 cm^2 approximately). All the potentials are reported in the SCE scale. Post-test analysis included examination in an optical stereomicroscope and scanning electron microscope (SEM).

3. Experimental Results and Discussion

Figure 1 shows the determination of the crevice corrosion repassivation of alloy HYBRID-BC1 in 5 mol/L CaCl$_2$ at 80 ºC. The crevice corrosion repassivation potential (Eco) for this technique is a cross-over potential determined at the intersection of the forward (stage 1) and reverse (stage 3) scans (Figure 1). Once the current density reached a predetermined value (2 or 20 µA/cm²), the controlling mode was switched from potentiodynamic to galvanostatic and the predetermined current density was applied for 2 hours. The current of the galvanostatic step was increased one order of magnitude depending on the resistance of each alloy in particular, the temperature or the presence of an anodic peak in the range of passivity. The galvanostatic current variation applied does not significantly affect the value of E$_{CO}$ (Rincón Ortíz, 2010).
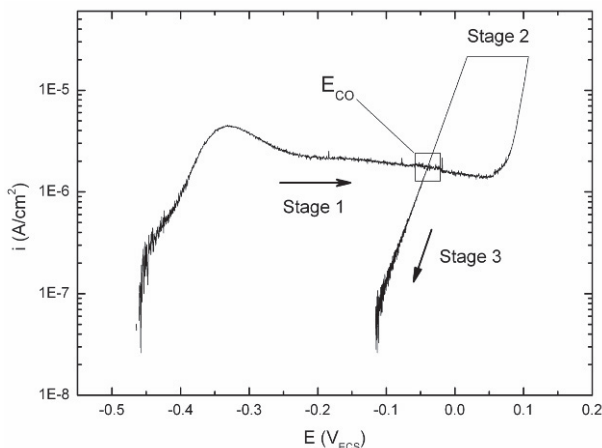

Figure 1. PD-GS-PD test for alloy HYBRID-BC1 in 5 mol/L CaCl$_2$ at 80 ºC.

Figure 2 shows the E$_{CO}$ obtained by the PD-GS-PD method as a function of temperature (T) for the tested alloys. The crevice corrosion resistance of the alloys increased in the following order: 625 < C-22 < C-22HS < HYBRID-BC1. The Mo content increased in the same order. Alloy HYBRID-BC1 suffered crevice corrosion at T $\geqslant$ 60 ºC. Alloys C-22 and C-22HS suffered crevice corrosion only at T $\geqslant$ 40 ºC. Alloy 625 suffered crevice corrosion in the whole studied T range, from 20 to 100 ºC. No tests were performed at temperatures below 20 °C, thus a lower limit of temperature for crevice corrosion of Alloy 625 could not be obtained. E$_{CO}$ decreased linearly with T for the tested alloys, as reported in the literature (Evans et al., 2005). The fit parameters obtained by linear least squares are listed in Table 2. Good correlation coefficients (R^2) were obtained in most of the cases. However, alloy 22 showed a low value of R^2 which was attributed to the use of specimens from different heats.

Table 2. Fit parameters for E_{CO} and R^2.

$E_{CO} = A\ T + B$	A (V/°C)	B(V_{ECS})	R^2
Alloy 625	-0,0029	-0,007	0,937
Alloy C-22	-0,0019	-0,005	0,694
Alloy C-22HS	-0,0025	0,068	0,911
Alloy HYBRID-BC1	-0,0022	0,135	0,969
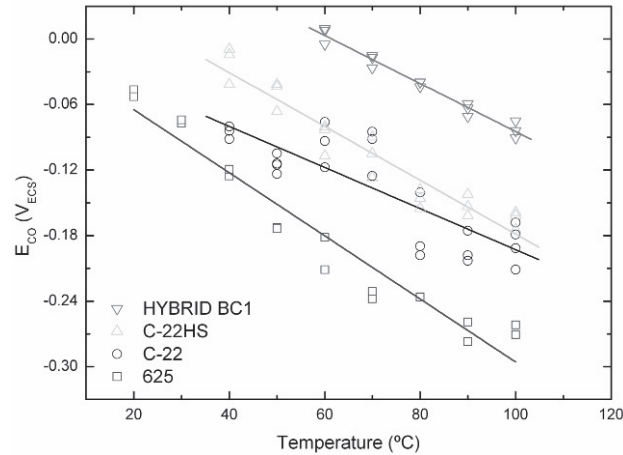
Figure 2. E_{CO} as a function of T for alloys 625, C-22, C-22HS and HYBRID-BC1 in CaCl$_2$ 5 mol/L. Symbols: data; lines: fit.

Figures 3 (a) and 3 (b) show crevice corrosion of alloy C-22HS tested in CaCl$_2$ 5 mol/L at 40°C. The attack started at the crevice former / metal interface and progressed outward towards the solution. The morphology observed in Figure 3 (b) is representative of the attack suffered by the four studied alloys at different temperatures.
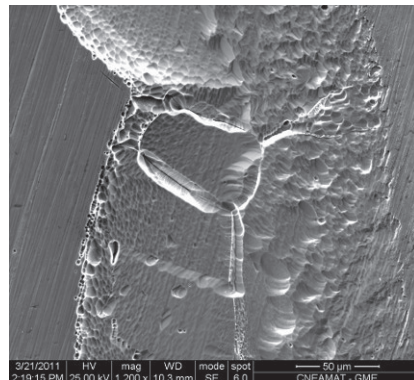

Figure 3 (a)

Figure 3 (b)

Fig. 3. (a) Crevice corrosion of Alloy C-22HS tested in CaCl$_2$ 5 mol/L at 40°C; (b) SEM image of the same specimen

The corrosion potential (E_{CORR}) of the alloys was measured in acidic solutions. These measurements were performed in 1 and 3 mol/L HCl solutions which simulate the conditions within active crevices. Figures 4 a-b shows E_{CORR} after 2 hours of immersion as a function of T. In 1 mol/L HCl solutions, E_{CORR} of the alloys slowly decreased as T increased, until it reached a relatively stable value. The standard deviation of E_{CORR} was of 10 mV. In 3 mol/L HCl solutions, E_{CORR} showed less variability with T. In general, E_{CORR} was higher in 3 mol/L HCl than in 1 mol/L HCl. Considering the T range from 50 to 100 ºC, alloy HYBRID-BC1 showed the highest E_{CORR} values, followed by alloy C-22HS and C-22. Alloy 625 showed the lowest E_{CORR} values, particularly in 1 M HCl.
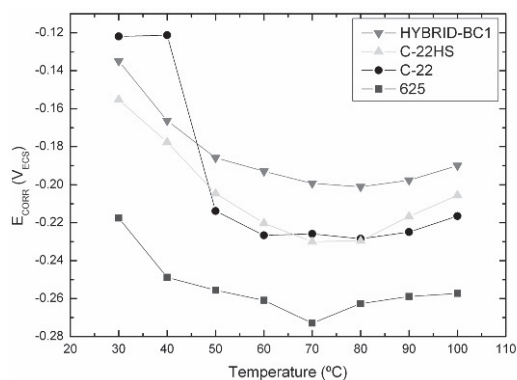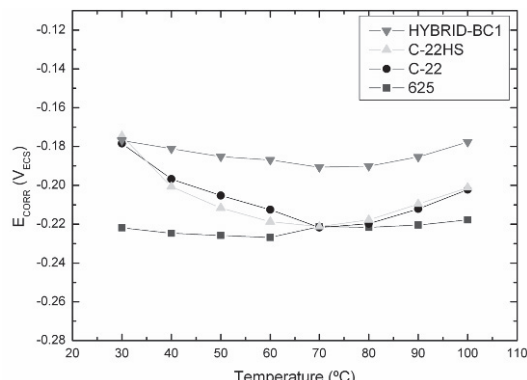

Figure 4 (a)   Figure 4 (b)

Fig. 4. (a) E_{CORR} as a function of T for the tested alloy in HCl 1mol/L solutions; (b) E_{CORR} as a function of T for the tested alloy in HCl 3 mol/L solutions

The localized acidification model states that the critical potential (in this case E_{CO}) is the sum of three contributions: the corrosion potential of the metal in the locally acidic solution (E_{CORR}^*), a polarization necessary to locally sustain the critical acidity (η) and the ohmic drop ($\Delta\Phi$) (Galvele and Duffó, 2006). This is stated in Equation 1.

$$E_{CO} = E_{CORR}^* + \eta + \Delta\Phi \qquad\qquad\qquad (1)$$

The terms $\eta + \Delta\Phi$ are negligible for sufficiently high chloride concentrations and temperatures. In these conditions Equation 1 becomes $E_{CO} = E_{CORR}^*$. This would be, from a theoretical viewpoint, the lowest potential at which the localized corrosion is able to proceed. The critical crevice solution is more aggressive as long as the considered alloy is more corrosion resistant (Szklarska-Smialowska, 2005; Combrade, 2000). In the present case, E_{CORR}^* was associated with the E_{CORR} values in 3 mol/L HCl for alloys HYBRID-BC1, C-22HS and C-22; while it was associated with those in 1 mol/L HCl for alloy 625. Figures 5 a-d shows the extrapolations at high temperatures of E_{CORR}^* and E_{CO} according to the fitting equations (Table 2). The objective of these extrapolations was to obtain the temperature at which $E_{CO} = E_{CORR}^*$, since $\eta + \Delta\Phi = 0$. The potential and temperature corresponding to the interceptions of E_{CO} and E_{CORR}^* for each alloy (Figures 5 a-d) are listed in Table 3. The extrapolation for alloy 625 lay within the studied range. The same for alloys C-22 and C-22HS indicated that T* was slightly above the studied T range; while T* for alloy HYBRID-BC1 was

far from the studied range. The potentials and temperatures listed in Table 3 are approximate values since they come from extrapolations.

Table 3. Values corresponding to the interceptions of E_{CO} and E_{CORR}^* in Figures 5 a-d

	$E_{CO} = E_{CORR}^*$ (V_{ECS})	Temperature (ºC)
Alloy 625	-0.261	88
Alloy C-22	-0.212	110
Alloy C-22HS	-0.214	115
Alloy HYBRID-BC1	-0.184	145

The potential values determined for each alloy in conditions where $\eta + \Delta\Phi \rightarrow 0$ are expected to be the lowest ones at which localized corrosion is able to proceed. If E_{CORR} of the alloys remained below $E_{CO} = E_{CORR}^*$ (Table 3), the material would not suffer any kind of localized attack (neither pitting nor crevice corrosion). Moreover, these potentials are independent of chloride concentration and temperature. These values may be used as strong parameters for assessing the localized corrosion susceptibility of materials in a long term timescale. The parameters determined in this study are relevant for applications of nickel alloys as engineered barriers of nuclear repositories.
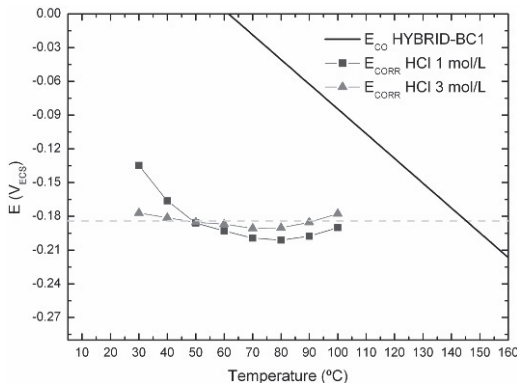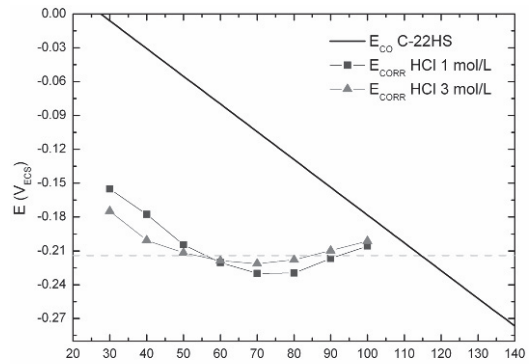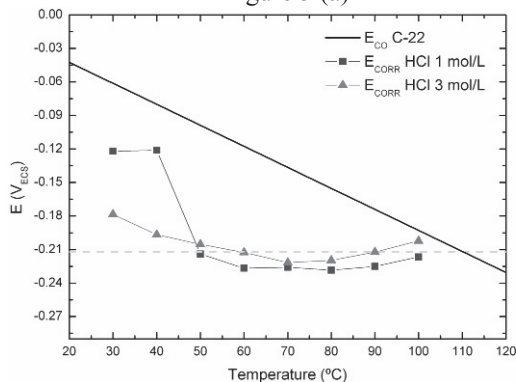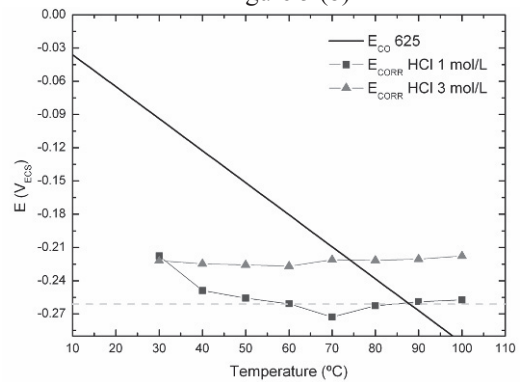

Figure 5 (a)

Figure 5 (b)

Figure 5 (c)

Figure 5 (d)

Fig. 5. (a) Extrapolation of E_{CO} and E_{CORR}^* for alloy HYBRID-BC1; (b) for alloy C-22HS; (c) for alloy C-22; (d) for alloy 625

4. Conclusions

1.   HYBRID-BC1 was the most resistant alloy to chloride-induced crevice corrosion, followed by alloys C-22HS, C-22 and 625. The localized corrosion resistance of these alloys increased with the Mo content.

2. E_{CO} showed a linear decrease with temperature.

3.   The lowest potentials at which the localized corrosion is able to proceed according to the localized acidification model were determined. The potentials and temperatures corresponding to these conditions were estimated by extrapolation. They were 0.184 V_{SCE} and 145 ºC for alloy HYBRID-BC1, -0.214 V_{SCE} and 115 ºC for alloy C-22HS, -0.212 V_{SCE} and 110 ºC for alloy C-22, and -0.261 V_{SCE} and 88 ºC for alloy 625.

4.   These extrapolated potentials are strong parameters for assessing the localized corrosion susceptibility of the materials in a long term timescale, since they are independent of temperature, chloride concentration, crevice mechanism, crevice former material and type, etc.

Acknowledgements

References

ASTM G48-03, 2003, "Standard Test Methods for Pitting and Crevice Corrosion Resistance of Stainless Steels and Related Alloys by Use of Ferric Chloride Solution" Annual Book of ASTM Standards, vol. 03.02 (West Conshohocken, PA: ASTM Intl., 2003), pp. 191-201.

ASTM G192-08, 2008, "Standard Test Method for Determining the Crevice Repassivation Potential of Corrosion-Resistant Alloys Using a Potentiodynamic-Galvanostatic-Potentiostatic Technique" Annual Book of ASTM Standards, vol. 03.02 (West Conshohocken, PA: ASTM Intl., 2008).

Combrade, P. 2000, Crevice corrosion of metallic materials in Corrosion mechanisms in theory and practice, Second edition, Marcus P. Editor, Marcel Dekker, pp. 349-397.

Evans, K. J., Yilmaz, A., Day, S. D., Wong, L. L. Estill, J. C., Rebak, R. B., 2005, Journal of Metals, p. 56.

Fontana, M., 1986, Corrosion Engineering, Third edition, McGraw-Hill.

Galvele, J. R., Duffó, G. S., 2006, Degradación de Materiales. Corrosión. Primera Edición, Jorge Baudino Ediciones, Instituto Sabato, Buenos Aires.

Gras, J. M., 2002, C. R. Physique 3, p. 891.

Mishra, A. K., Frankel, G. S., 2008, Corrosion, Vol. 64, Nº 11, p. 836.

Rebak, R. B., 2000, Materials science and technology. A comprehensive treatment. Corrosion and environmental degradation, Vol. II, pp. 69-111, Schuntze M., Editor, Wiley, VCH.

Rincón Ortíz, M., Rodríguez, M. A., Carranza, R. M., Rebak, R. B., 2010, Corrosion, Vol. 66, Nº 10.

Szklarska-Smialowska, Z., 2005 Pitting and Crevice Corrosion, NACE International.

Valen, S., Gartland, P. O., 1995, Corrosion, Vol. 51, Nº. 10, p. 750.

Whiterspoon, P. A., Bodvarsson, G. S., 2001, Geological Challenges in Radioactive Waste Isolation, Third Worldwide Review, University of California, Berkeley, CA, USA.